Simulation of Flow Characteristics of Refrigerant inside Adiabatic Straight Capillary Tube

Shivkumar [1]*, Omprakash Hebbal [2]
1*PG Student, Thermal power Engineering, PDA College of Engineering, Gulbarga-585102, Karnataka (INDIA)
2Professors, Department of Mechanical Engineering, PDA College of Engineering, Gulbarga-585102, Karnataka (INDIA)

Abstract

In the present investigation, an attempt is made to develop mathematical model to determine the flow characteristics of refrigerant inside a straight capillary tube for adiabatic flow conditions. The proposed model can predict the length of the adiabatic straight capillary tube for a given mass flow rate. In the present study R-12 has been used as a working fluid inside the straight capillary tube of diameter 1.17 mm and 1.41 mm and used the same model to study the flow characteristics of refrigerant in ANSYS CFX software.

Finally the results of mathematical model are valuated with ANSYS CFX and the results are found to be in fair agreement.

Key word: adiabatic straight capillary tube, refrigerant R12, ICEM, CFD AND ANSYS CFX.

1. INTRODUCTION

The capillary tube is simple, reliable, inexpensive, and widely used as a throttling device in this small-scale vapor compression refrigeration appliances. It is used as an automatic flow rate controller for the refrigerant when varying load conditions and varying condenser and evaporator temperatures are to be encountered. The capillary tube is employed where the cooling load is fairly constant and the cooling capacity is not more than 3TR (ton of refrigerant). Capillary tube is a long narrow hollow drawn copper tube with an internal diameter ranging from 0.5 to 2.0 mm. Capillary tubes have been investigated in detail for many decades.A capillary tube is a common expansion device used in small sized refrigeration and air-conditioning systems. A capillary tube is a constant area expansion device used in a vapor-compression refrigeration system located between the condenser and the evaporator and whose function is to reduce the high pressure in the condenser to low pressure in the evaporator. The capillary tube expansion devices are widely used in refrigeration equipment, especially in small units such as household refrigerators, freezers and small air conditioners. The thermo dynamical analysis of capillary tube though looking simple is complicated because of irreversibility. As already indicated it is experimentally studied by various researches [8] and reported. To evaluate heat transfer and fluid flow characteristics of expanses model. The numerical simulation has been done by some researches [5] and presented. The refrigerants used for the numerical analysis R22, R134a, R600a, R407c and R410a. Further analysis heat transfer and fluid flow characteristics studied of capillary tube R12 using CFD that is ANSYS CFX carried out and presented this project .In continuous with this the results obtained various research are compared and presented.

2. METHODOLOGY

The physical domain has been converted to computational domain, as shown in Figure.3.1. The refrigerant from condenser enters the capillary tube at section 1 in a sub cooled liquid state. Due to sudden contraction at the capillary tube inlet, the refrigerant pressure is dropped and state point 2 is reached. Subsequently, a single phase liquid flow in the capillary tube is established. Since the flow of refrigerant through the capillary tube is adiabatic, the temperature of the flowing liquid refrigerant remains constant. The pressure inside the capillary tube drops linearly as long as the flow is in liquid state. When the refrigerant pressure drops up to point 3 i.e., the saturation pressure, at that point two-phase flow set up in the capillary tube. In the two-phase region of the capillary tube, the temperature and pressure of refrigerant starts falling rapidly till the evaporator pressure or the choking point 4 is attained.

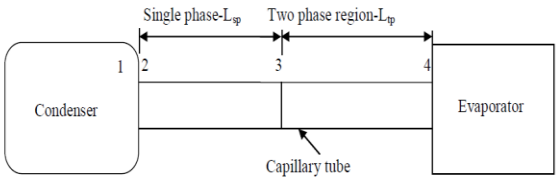

Fig. Computational domain of adiabatic straight capillary tube

Thus, the flow of refrigerant through an adiabatic straight capillary tube has been divided into following two distinct regions:

1 – 2 represents pressure drop due to
sudden contraction at capillary inlet,
2 – 3 represents single-phase subcooled
flow region.
3 – 4 represents liquid-vapour two-phase flow region.
Consider an infinitesimal fluid element of length 'dL' within the capillary tube, shown in Figure 3.2 , and applying the equations of conservation of mass, momentum and energy are expressed in equations .

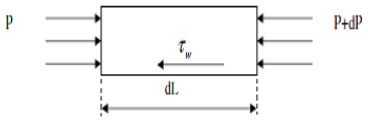

Fig. Forces acting on the fluid element

Mass Balance

Application of continuity equation results into the following

$$m = \rho V \quad \text{or} \quad G = \frac{m}{A} = \rho V$$

Momentum Balance

On applying the principle of momentum conservation or the Second law of Thermodynamics, the following equation will result

$$P.A - (P + dP).A - \tau_w(\pi d)dL = mdV$$

On simplification, Equation 3.2 reduces to

$$-dP = \frac{f}{2d}\rho V^2 dL + \rho V dV$$

Taking log both sides of equation 3.1 and then differentiating and simplifying

$$-\frac{dV}{V} = \frac{d\rho}{\rho}$$

Equation 3.3 reduces to

$$dL = \frac{2d}{f}\left(\frac{\rho dP}{G^2} - \frac{d\rho}{\rho}\right)$$

Energy Balance

On applying the steady flow energy equation on the element to get

$$\delta q - \delta w = dh + VdV + gdZ$$

2.1 Single-phase region

In the single phase liquid region, the refrigerant density is almost constant as the liquids are practically incompressible (ρ = constant) and with tube cross sectional area being constant, from mass balance represented by Equation, the velocity is constant. Integrating Equation, the length of single-phase liquid region expressed in equations.

$$L_{sp} = \frac{d}{f_{sp}}\left(\frac{2}{\rho V^2}(P_2 - P_3)\right) = \frac{2d\rho(P_2 - P_3)}{fG^2}$$

Pressure loss due to entrance effects

$$P_1 - P_2 = k\frac{\rho V^2}{2}$$

Where k is the entrance loss coefficient, taken as 1.5

From equations.

$$L_{sp} = \frac{d}{f_{sp}}\left[\frac{2\rho}{G^2}(P_1 - P_3) - k\right]$$

Where 'fsp' is the single phase friction factor .

2.2 Two-phase regions

Two-phase region expressed in equations .

Applying continuity equation between sections 3 and 4

$$h_3 + \frac{V_3^2}{2} = h_f + x h_{fg} + \frac{G^2}{2}(v_f + x v_{fg})^2$$

$$x = \frac{-h_{fg} - G^2 v_f v_{fg} + \sqrt{(G^2 v_f v_{fg})^2 - 2G^2 v_{fg}^2\left(\frac{G^2 v_f^2}{2} - h_4 - \frac{v_3}{2} + h_f\right)}}{G^2 v_{fg}^2}$$

Equation is quadratic in x and the quality x can be expressed as

The two-phase friction factor ftp can be calculated using Moody's correlation [28]. The Reynolds number in two-phase region has to be determined by

$$Re_{tp} = \frac{Vd}{\mu_{tp} v_{tp}}$$

Where, μ_{tp} is the two-phase dynamic viscosity correlations

Finite Volume Formulation

ANSYS-CFX uses a finite-element-based finite volume method. The governing equations namely the conservation for mass; momentum and energy are expressed in equations.

$$\frac{\partial \rho}{\partial t} + \frac{\partial}{\partial x_j}(\rho u_j) = 0$$

$$\frac{\partial}{\partial t}(\rho u_i) + \frac{\partial}{\partial x_j}(\rho u_j u_i) = -\frac{\partial P}{\partial x_i} + \frac{\partial}{\partial x_j}\left[\mu_{eff}\left(\frac{\partial u_i}{\partial x_j} + \frac{\partial u_j}{\partial x_i}\right)\right] + S_{ui}$$

$$\frac{\partial}{\partial t}(\rho\phi) + \frac{\partial}{\partial x_j}(\rho u_j \phi) = \frac{\partial}{\partial x_j}\left[\Gamma_{eff}\left(\frac{\partial \phi}{\partial x_j}\right)\right] + S_\phi$$

Where the energy conservation has been replaced by a generic scalar transport equation. The finite volume method proceeds by integrating these equations over a fixed control volume, which, using Gauss Theorem, results in equation.

$$\frac{\partial}{\partial t}\int_v \rho dv + \int_s \rho u_j dn_j = 0$$

$$\frac{\partial}{\partial t}\int_v \rho u_i dv + \int_s \rho u_j u_i dn_j = -\int_s P dn_i + \int_s \mu_{eff}\left(\frac{\partial u_i}{\partial x_j} + \frac{\partial u_j}{\partial x_i}\right)dn_j + \int_v S_{ui} dv$$

$$\frac{\partial}{\partial t}\int_v \rho\phi dv + \int_s \rho u_j \phi dn_j = \int_s \Gamma_{eff}\left(\frac{\partial \phi}{\partial x_j}\right)dn_j + \int_v S_\phi dv$$

where v and s denote volume and surface integrals respectively and dn_jrepresents the differential Cartesian component of the outward normal surface vector.

The equations represent a flux balance in a control volume. The above equations are applied to each control volume or cell in the

computational domain. These continuous equations are approximated numerically using discrete functions. Discretisation of the equations yields the following in equations.

3. Modelling

For setting up any CFD problem, the geometry has to be modelled with required details, mesh has to be generated optimally to obtain the results correctly and flow parameters and boundary conditions are to be set up for solving the problem. The discretized domain is solved using solver and results are analysed in post processor. In the present investigation, ICEM software and ANSYS-CFX software is used for the geometry modelling and mesh generation. ANSYS-CFX software issued for defining boundary conditions, solving and post processing.

$$\rho V\left(\frac{\rho-\rho^{o}}{\Delta t}\right)+\sum_{ip}\left(\rho u_j \Delta n_j\right)_{ip}=0$$

$$\rho V\left(\frac{u_i-u_i^{o}}{\Delta t}\right)+\sum_{ip}\dot{m}_{ip}\left(u_i\right)_{ip}=\sum_{ip}\left(P\Delta n_i\right)_{ip}+\sum_{ip}\left(\mu_{eff}\left(\frac{\partial u_i}{\partial x_j}+\frac{\partial u_j}{\partial x_i}\right)\Delta n_j\right)_{ip}+\bar{S}_{u_i}V$$

$$\rho V\left(\frac{\phi_i-\phi^{o}}{\Delta t}\right)+\sum_{ip}\dot{m}_{ip}\phi_{ip}=\sum_{ip}\left(\Gamma_{eff}\frac{\partial\phi}{\partial x_j}\Delta n_j\right)_{ip}+\bar{S}_{\phi}V$$

Where $\dot{m}_{ip}=(\rho u_j \Delta n_j)^{o}_{ip}$,

V is volume of the control volume

3.1 Modelling

For setting up any CFD problem, the geometry has to be modelled with required details, mesh has to be generated optimally to obtain the results correctly and flow parameters and boundary conditions are to be set up for solving the problem. The discretized domain is solved using solver and results are analysed in post processor. In the present investigation, CAD model and ANSYS-CFX software is used for the geometry modelling and mesh generation. ANSYS-CFX software issued for defining boundary conditions, solving and post processing.

3.2 Geometry and mesh generation

In order to use simulation techniques developed, a physical model is used in ICEM 13.0 software.

After creation of the physical model, file is saved in *.iges format.

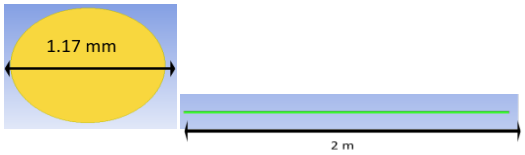

Fig.Straight capillary tube model for case 1

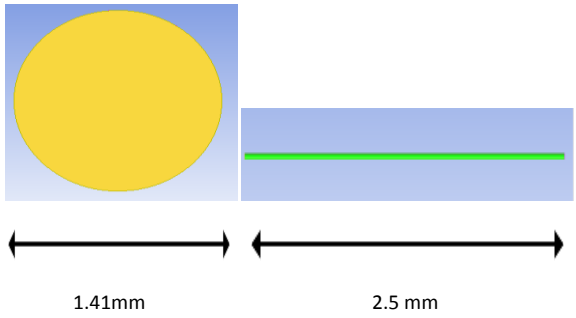

Fig. Straight capillary tube model for case 2

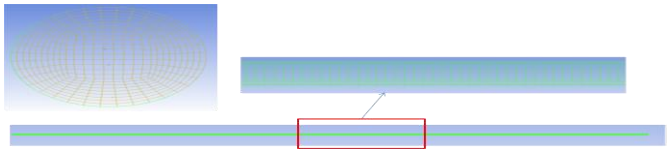

No of elements =1,45,000

Figure Meshing for case 1

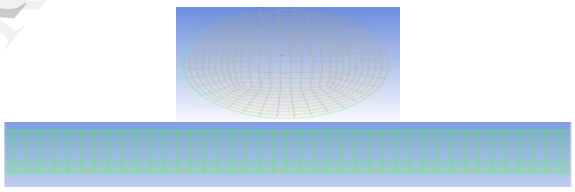

No of elements =1,40,000

Fig. Meshing for case 2

Now open the ANSYS Workbench and open the meshing module for creation of CFX mesh. Set the physical preference as CFD and mesh method as CFX. Import the geometry in the ANSYS Workbench, by clicking on the tab geometry and from this tab select from file. A new window CFX mesh is opened. Now set the default body spacing and default face spacing as the size of the capillary tube used is small reduce the size of default body spacing and default face spacing. The meshing is done by iterative process. If a very fine mesh is created then more calculation work is to be done by the processor. Generate the volume mesh by clicking on generate volume mesh. file is saved in *.gtm or *.After creation of CFX mesh, open ANSYS CFX module. In the ANSYS CFX open CFX-Pre and from the file menu select new simulation and set the simulation type as general

3.3 ANSYS-CFX SETUP

The first steps taken after importing the mesh geometry into ANSYS-CFX involve checking the mesh/grid for errors. Checking the grid assures that all zones are present and all dimensions are correct. It is also important to check the volume and make sure that it is not negative. If the volume is shown as negative, there is a problem with the grid. When the grid is checked completely and free of errors, a scale and units can be assigned. For this study, the grid was created in mm, and then scaled to meters. Once the grid was set, the solver and boundary conditions of the system were then set and cases were run and analyzed.

3.4 Simulation with ANSYS CFX

An ANSYS CFX analysis consists of several main steps:

3.4.1 Define the Problem Domain

We have to first of all define the proper domain for each problem to analyze and then apply the boundaries of the problem where conditions are known.

3.4.2 Define the Flow Regime

In this step, the character of the flow is defined, as the character is a function of the fluid properties, geometry, and the approximate magnitude of the velocity field. Fluid flow problems that ANSYS CFX solves will include gases and liquids, the properties of which can vary significantly with temperature. The flow of gases is restricted to ideal gases. So it is very important to determine whether the effect of temperature on fluid density, viscosity, and thermal conductivity. As in many cases, we can get adequate results with constant properties. To assess whether we need the ANSYS CFX turbulence model, use an estimate of the Reynolds number, which measures the relative strengths of the inertial and viscous forces.

To determine whether we need to use the compressible flow option, estimate the Mach number. As the Mach number at any point in the flow field is the ratio of the fluid speed and the speed of sound. At Mach numbers above approximately 0.3, consider using the compressible solution. At Mach numbers above approximately 0.7, we can expect significant differences between incompressible and compressible results.

3.4.3 Creating the Finite Element Mesh

We have to make assumptions about where the gradients are expected to be the highest, and adjust the mesh accordingly. Now let us consider if we are using the turbulence model, then the region near the walls must have a much denser mesh than that would be needed for a laminar flow.

We have to use hexahedral elements to capture detail in high-gradient regions and tetrahedral elements in less critical regions. Although we can instruct ANSYS to automatically create pyramid elements at the interface. For two phase flow analysis, especially turbulent, we should not to use pyramid elements in the region near the walls because it may lead to inaccuracies in the solution

3.4.4 Applying Boundary Conditions

After creating CFX mesh for the problem to be analyzed we have to apply the boundary conditions for the problem that we can done before or after creation of the CFX mesh. We have to define the boundary condition for the each element in the problem. Table 4.1 boundary conditions, if we not able to properly define specified condition for a dependent variable, a zero gradient of that value normal to the surface is assumed. We have no need to restart the ANSYS CFX analysis if we forgot to apply the boundary condition accidentally because we can change the boundary condition unless the change causes instabilities in the analysis solution.

Table 4.1 Boundary Conditions

S. No.	Input Parameters	Case 1	Case 2
1	Refrigerant Used	R12	R12
2	Mass flow rate	15.66 kg/h	21.23kg/h
3	Dia of Capillary Tube	1.17 mm	1.41 mm
4	Roughness Ratio	0.003	0.000384
5	Capillary TubeInlet Pressure	885 kPa	858 kPa
6	Capillary Tube Inlet Temperature	303k	305.8k
7	Capillary Tube Length	2m	2.5m

3.4.5 Setting ANSYS CFX Analysis Parameters

In order to use the solution of the temperature equation for the two phase region, we must have to activate and the behavior of relevant dependent variables. These variables include velocity, pressure, and temperature. An analysis typically requires multiple restarts.

3.4.6 Solve the Problem

We have to observe the convergence of solution and stability of the analysis by observing the rate of change of the solution and the behavior of relevant dependent variables. These variables include velocity, pressure, and temperature.

3.4.7 Examine the Results

After the solution run by the ANSYS CFX we have to run the post processor to get the output results in the form of graphs, for this we have to define the stream line which acts as reference to draw graphs.

4. RESULTS AND DISCUSSION

4.1 Validating the Results

Results obtained from the proposed model with experimental data.

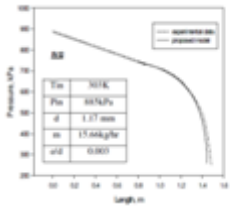

Case1

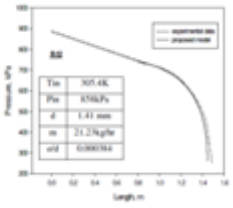

Case 2

Fig.4.1 a) Comparison of proposed model with experimental data Li et al. (23).

b) Comparison of proposed model with experimental data Mikol et al. (26).

These experiment results are compared with result generated by the model proposed for R12.The comparison indicated earlier shown in fig.4.1a for Li etal.(18)results and fig.4.1b for mikol et al.(19) results.

The proposed model under predicts the capillary length by 2.7 percent for Li et al. [23] experimental data generated for the flow of R-12. However, the proposed model is in good agreement with the data of Li et al. [23].In the figure 4.1b the capillary tube length for the proposed model under predicts the experimental data of Mikol et al. [26] by 3.4 percent. However, the proposed model is in good agreement with the data of Mikol et al.[26].

4.2 Simulation of refrigerant R-12

Case 01

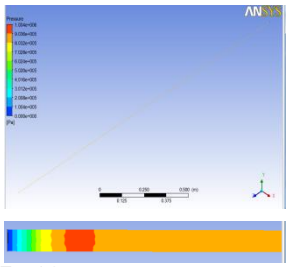

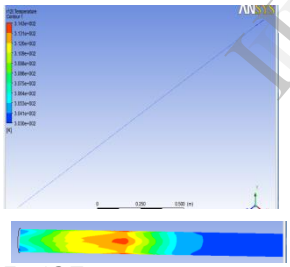

Fig.4.2 pressure contours

Fig.4.3 Temperature contours

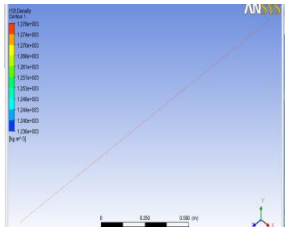

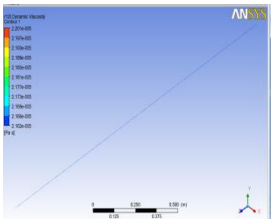

Fig.4.4 Density contours

Fig.4.5 Viscosity contours

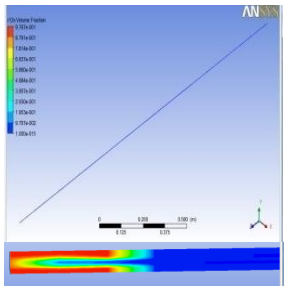

Fig.4.6 Volume fraction contours

Case :02

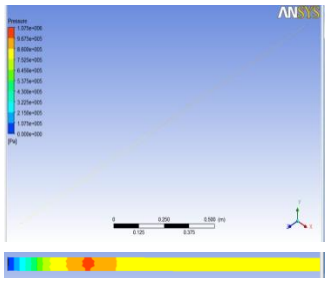

Fig.4.7 Pressurecontours

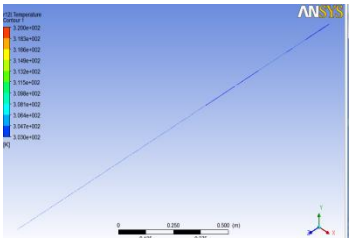

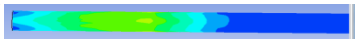

Fig.4.8 Temperature contours

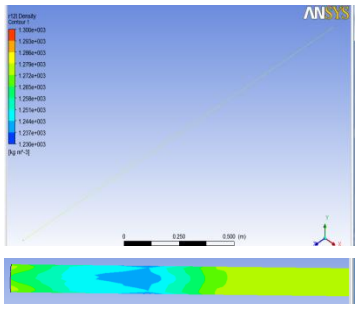

Fig.4.9 Density contours

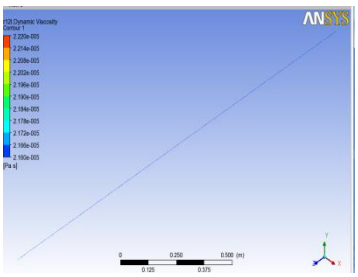

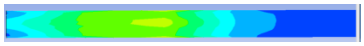

Fig.4.10 Viscosity contours

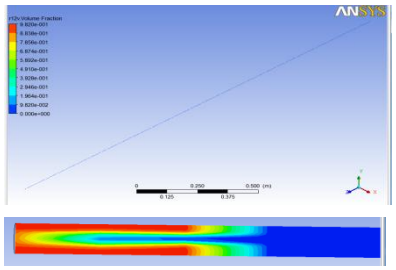

Fig.4.11 Volume fraction

Fig.4.2, 4.3, 4.4, 4.5 and 4.6.shows the pressure contours temperature, density, viscosity and volume fraction contours of case1 using ANSYS CFX.

SimilarlyFig.4.7, 4.8, 4.9, 4.10 and 4.11 shows the pressure and temperature density viscosity and volume fraction contours of case2 studied. As it is expected from the fig. we can absorbed that the pressure drop, temperature, density decreases and viscosity increases along the length of the capillary tube.

Using visual c++ code the pressure contour, temperature, Reynolds number, viscosity, density and specific volume across the length of the capillary tube is generated and same in presented in appendex1. Part A of the appendix presents visual c++ program code case1 and case2 respectively. Table A.1 and A.2 of part B indicates results obtained visual c++ code case1 and case2 respectively. These tabulated values are also presented in the form of graph and results are compared with ANSYS CFX.

4.3 Graphs

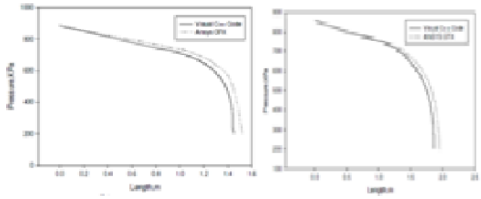

Case 1 Case 2

Fig. 4.12 Pressure and length plot for proposed model with ANSYS CFX

Figure 4.12shows the variation of pressure across the length proposed model with ANSYS CFX. For case1 and case2 as expected pressure reduces through its length as shown. The results are found to be fair agreement from ANSYS CFX with respect to the visual c++ code for case1and case2. For the given Pressure drop for (case 1)635kPa and (case2)618kPa,the expected length is 1.4491m for visual c++ code and 1.519m ANSYS CFX for R12.Similarly for case2 the expected length is1.867 mfor visual c++ code and is 1.9490 m ANSYS CFX for R12.

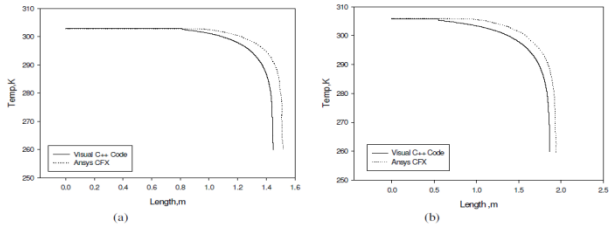

Figure 4.13 Temperature and length plot for proposed model with ANSYS CFX

Figure 4.13shows the variation of temperature across the length proposed model with ANSYS CFX. For case1 and case2 as expected temperature reduces through its length as shown. The results are found to be fair agreement from ANSYS CFX with respect to the visual c++ code for case1 and case2. For the given Temperature drop for(case 1) 43K and(case 2) 45.8K,the expected length is 1.4491m for visual c++ code and 1.519m ANSYS CFX for R12. Similarly for case2 the expected length is1.867 m for visual c++ code and is 1.9490mANSYS CFX forR12.

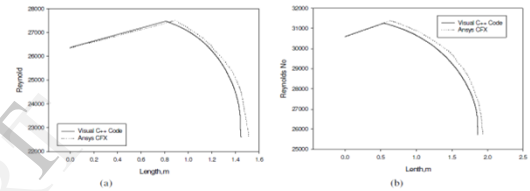

Case 1 Case 2

Fig. 4.14 Reynolds number and length plot for proposed model with ANSYS C

Figure 4.14 shows the variation of Reynolds number across the length proposed model with ANSYS CFX. For case1 and case b as expected Reynolds number reduces through its length as shown. The results are found to be fair agreement from ANSYS CFX with respect to the visual c++ code for case1and case2. For the given Reynolds number drop (case a) 3400 and 4550(case 2), the expected length is 1.4491m for visual c++ code and 1.519m ANSYS CFX for R12 .similarly for case2 the expected length is1.867mfor visual c++ code and is 1.9490m ANSYS CFX for R12.

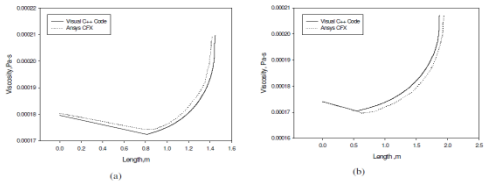

Fig. 4.15 shows the variation of viscosity across the length proposed model with ANSYS CFX. For case1 and case2 as expected viscosity increment through its length as shown. The

results are found to be fair agreement from ANSYS CFX with respect to the visual c++ code for case1and case2. For the given Viscosity increment (case 1) 0.00003Pa-s and (case 2) 0.000075Pa-s,the expected length is 1.4491 m for visual c++ code and 1.519 m ANSYS CFX for R12.Similarly for case2 the expected length is1.867m for visual c++ code and 1.9490 m ANSYS CFX for R12

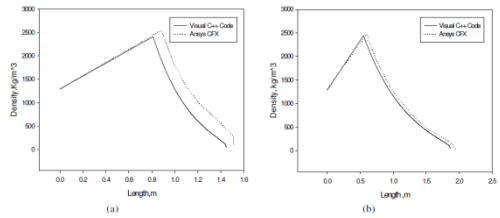

Fig. 4.16 Density and length plot for proposed model with ANSYS CFX

Figure 4.16 shows the variation of density across the length proposed model with ANSYS CFX. For case1 and case2 as expected density reduces through its length as shown. The results are found to be fair agreement from ANSYS CFX with respect to the visual c++ code for case1and case2. For the given density drop for (case 1)1248 kg/m^3 and (case 2)1300kg/$m^3$the expected length is 1.4491m for visual c++ code and 1.519 m ANSYS CFX for R12 .similarly for case2 the expected length is1.867m for visual c++ code and is 1.9490m ANSYS CFX for R12.

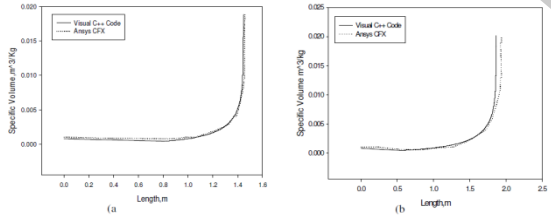

Figu. 4.17 Specific volume and length plot for proposed model with ANSYS CFX

Figure 4.17 shows the variation of specific volume across the length proposed model with ANSYS CFX. For case1 and case2 as expected Specific volume increment through its length as shown. The results are found to be fair agreement from ANSYS CFX with respect to the visual c++ code for case1and case2. For the given specific Specific volume increment (case 1) 0.018m^3/kg and (case 2) 0.02 m^3/kg,the expected length is 1.449m for visual c++ code and 1.519m ANSYS CFX for R12 .similarly for case2 the expected length is1.867m for visual c++ code and is 1.9490m ANSYS CFX for R12.

5. CONCLUSION

The following conclusion can be drawn.

- Model is created for the straight capillary tube of length 2m and 2.5m for the modelling is done.
- A numerical solution visual c++ code generated and presented.
- The CFD simulation for the consider straight capillary tube done ANSYS CFX and presented.
- The variation of pressure drop, temperature drop, Reynolds number drop and density drop are compared for the case1 and case2 using visual c++ code and ANSYS CFX. The results obtained both well comparable with a small 2 to 3% of error.
- The viscosity and specific volume increment are compared for the case1 and case2 using visual c++ code and ANSYS CFX. The results obtained both well comparable with a small 2 to 3% of error.

REFERENCE

1 S. G. Kim. Experimental investigation of the performance of R22, R407C and R410A in several capillary tubes for air-conditioners. International Journal of Refrigeration 25 (2002) 521–531,2002 Elsevier Science Ltd.

2 Thamir K. Salim. The Effect of the Capillary Tube Coil Number on the Refrigeration System Performance. Tikrit Journal of Engineering Sciences/Vol.19/No.2/June 2012, (18-29)

3 L. B. Ortiz, S. Y. Motta, S. L. Braga. “Experimental analysis of adiabatic flow of non- azeotropic mixture R-407c through a capillary tube” EngenhariaTermica, No. 1, pp. 41-46.

4 *Krishna reddy Venna*.non-adiabatic & adiabatic flow of r 410a through spiral capillary tubes: an experimental evaluation, International Journal of Materials, Manufacturing and Design (IJMMD)

5 Chang Nyeun Kim & Young Moo Park, “ Investigation on the Selection of Capillary Tube for the Alternative Refrigerant R-407C,” International Journal of Air-Conditioning and Refrigeration Volume 8, May (2000), pp.40-49.

6 Melo, C., Ferreira, R. T. S., Neto, C. B., Goncalves, J. M., and Mezavila. M.M., 1999, “An Experimental Analysis of Adiabatic Capillary Tubes,” Appl. Therm. Eng., 19(6), pp. 669–684.

7 Sami, S. M., Maltais, H. and Desjardins, D. E., Influence of Geometrical Parameters on Capillary

Behavior with New Alternative Refrigerants, Mechanical Engineering, School of Engineering University of Moncton, Moncton, NB, E1A3E9.

8 Akure, Ondo State, Nigeria, Effect of Coiled Capillary Tube Pitch on Vapour Compression Refrigeration System Performance, AU J.T. 11(1), p 14-22, Jul.2007.

9 Bansal, P.K. and Rupasinghe, A.S., An Empirical Model for Sizing Capillary Tubes, *Int. J. Refrigeration*, 19, p 497 –505, 1996.

10 Bansal, P.K. and Rupasinghe, A.S., A Homogenous Model for AdiabaticCapillary Tubes, Applied *Thermal Engineering*, Vol. 18, Nos.3-4, pp. 207 –219,1998.

11 Wongwises, S., Songnetichaovalit, T., Lokathada, N., Kritsadathikaran, P.,Suchatawat, M. and Pirompak, W. A comparison of the flow characteristics of refrigerants flowing through adiabatic capillary tubes, *Int. Comm. Heat Mass Transfer*, Vol. 27, No. 5, pp. 611-621, 2000.

12 Wongwises, S. and Pirompak, W., Flow Characteristics of Pure Refrigerants and Refrigerant Mixtures in Adiabatic Capillary Tubes, *Applied Thermal Engineering*, Vol. 21, pp. 845-861, 2001

13 Bansal, P.K. and Wang, G., Numerical analysis of choked refrigerant flow in adiabatic capillary tubes *Applied Thermal Engineering*, Vol. 25, pp. 2014-2028, 2003.

14 Zhang, C.L. and Ding, G.L., Approximate analytic solutions of adiabatic capillary tube, *Int. J. Refrigeration*, Vol. 27, pp. 17-24, 2004.

15 Khan, M.K., Kumar, R., Sahoo, P.K., 2007. Flow Characteristics of Refrigerants Flowing inside an Adiabatic Spiral Capillary Tube, *HVAC&R Research ASHRAE*, Vol. 13, issue 5, pp. 731-748

16 Khan, M.K., Kumar, R., Sahoo, P.K., Flow Characteristics of Refrigerants Flowing through Capillary Tubes - A Review, *Applied Thermal Engineering*, 2008 (available online on http://sciencedirect.com)

17 Khan, M.K., Kumar, R., Sahoo, P.K., 2008. A Homogenous Flow Model for Adiabatic Helical Capillary Tube, *ASHRAE Transactions*, Vol. 114, Part 1, pp.239-249

18 Colebrook, C.F., Turbulent Flow in Pipes with Particular Reference to theTransition Region between the Smooth and Rough Pipes Laws, *J. Inst. Civ. Eng.*,Vol. 11, pp. 133-156, 1939.

19 Beattie, D.R.H. and Whalley, P.B., A Simple Two-Phase Flow Model Frictional Pressure Drop in Two-Phase Flow Pressure Drop Calculation Method.*Int. J. Multiphase Flow*, vol.8, pp. 83-87, 1981.

20 Bittle R.R., Oliver J.V., Carter J.A., Extended Insightsinto the Metastable Liquid Region Behavoir in an Adiabatic Capillary Tube, *HVAC&R Research*, Vol 7, no.2, p107-123, 2001

21 Blassius, DasAhnlichkeitsgesetzbeiReibungsvorgangen in Flussigkeiten, *Forchg.Arb.Ing.-Wes.*, No. 131, Berlin, 1913Dean, W. R., Note on the Motion of Fluid in a Curved Pipe, *Phil. Mag.*, Vol.4,pp.208223,192

22 Cicchitti, A.E., Lombardi, C., Silvestri, M., Soldaini, J.and Zavattarelli, R., Two-Phase Cooling Experiments Pressure Drop, Heat Transfer and Burnout Measurements, *Energia Nucleare*, Vol.7, pp. 407-425, 1960.

23 Lin, S., Kwok, C.C.K., Li, R.Y., Chen, Z.H., and Chen,Z.Y., Local Frictional Pressure Drop During Vaporization of R12 through Capillary Tubes, *Int. J.Multiphase Flow*, Vol.17, pp. 83-87, 19917.

24 Chen, Z.H., Li, R.Y., Lin, S. and Chen, Z.Y., A Correlation for Meta stable Flow of R-12 through Capillary Tubes, *ASHRAE Trans.*, Vol. 96, pp. 550-554,1990.

25 Churchill, S.W., Frictional Equation Spans in all Fluid Flow Regimes, *Chemical Engineering*, Vol. 84: pp. 91-92, 1977.

26 Mikol, E.P., Adiabatic Single and Two-Phase Flow in Small Bore Tubes,ASHRAE Journal Vol. 5, p 75-86, 1963.

27 Dunn W., Meyer J.J., New Insights into the Behavoir of the Metastable Region of the Operating Capillary Tube, *HVAC&R Research*, Vol 4, no.1, p105-115, 1998

28 Dukler, A.E., Wicks, M. and Cleveland, R.G., Frictional Pressure Drop in Two-Phase Flow Part A and B, *AIChE Journal*, Vol. 10, pp. 38-51, 1964.

29 McAdams, W.H., Wood, W.K. and Bryan, R.L, Vaporization inside Horizontal Tubes- Part II: Benzene-Oil Mixture, *Trans. ASME*, Vol. 64, p. 193, 1942.

30 Moody, L.F., Friction Factors for Pipe Flow, *ASME*, Vol. 66, pp. 671-684, 1944.

31 Wong, T.N. and Ooi, K.T., Refrigerant Flow in Capillary Tube: An Assessment of the Two-Phase Viscosity Correlations on Model Prediction, *Int. Comm. Heat Mass Transfer*, Vol.22, No.4, pp. 595 –604, 1995.